

COMPUTED VERSUS OBSERVED INELASTIC SEISMIC RESPONSE OF LOW-RISE R/C SHEAR WALLS WITH BOUNDARY ELEMENTS

N ILE¹, J M REYNOUARD², F FLEURY³ And D CHAUVEL⁴

SUMMARY

Under the SAFE research project between Electricite de France (EDF-SEPTEN), COGEMA and the Joint Research Centre of Ispra (JRC) a series of pseudodynamic tests on various low-rise reinforced concrete shear walls were conducted at the ELSA reaction wall of JRC. This study involves the comparison of experimental PSD response data with results obtained from 2-D dynamic non-linear FEM time-history analysis. Towards the analysis of the damage and behaviour of shear walls subjected to earthquakes, a cyclic concrete model developed at INSA of Lyon is used. The model adopts the concept of a smeared crack approach with orthogonal fixed cracks and assumes a plane stress condition. The ability of the concrete model to reproduce the most important characteristics of the dynamic behaviour of this type of structural element was evaluated by comparison with available experimental data. The numerical results showed good correlation between the predicted and the actual response, global as well as local response being reasonable close to the experimental one.

INTRODUCTION

A great deal of research has been developed for low-rise shear walls for determining the ultimate capacity of the walls, stiffness reduction, or behaviour under cyclic loading. However, the research results do not provide sufficient information on the seismic behaviour of low-rise shear walls subjected to shear loading, with which to develop large and small-amplitude hysteretic rules for earthquake response studies. In many nuclear power plant buildings, reinforced concrete shear walls constitute a large percentage of total construction. Therefore, experimental and numerical studies are needed to improve mathematical models for non-linear dynamic analysis. Under the SAFE research project between Electricite de France (EDF-SEPTEN), COGEMA and the Joint Research Centre of Ispra (JRC) a series of pseudodynamic tests on various reinforced concrete shear walls were conducted at the ELSA reaction wall of JRC. The differences between each series of tests are related to the steel ratio of reinforcement, the natural frequency of the wall and the vertical loading. In order to achieve a good compromise between simplicity and accuracy a cyclic concrete model that simulates the most characteristic features of reinforced concrete under cyclic loading is proposed. The concrete model is of the type « fixed distributed cracks » with a possible double cracking only at 90°. The objective of this study is to assess the general applicability as well as the limitations of the present model in simulating the non-linear behaviour of a shear wall structure subjected to a large number of cycles.

EXPERIMENTAL PROGRAM

The SAFE experimental test programme [Pegon et al., 1998] involved the pseudodynamic testing of a series of 13 reinforced concrete shear wall specimens. The shear wall specimen (Figure 1) consisted of an « I » shaped wall system, as viewed in plan, inserted between a top and a base rigid beam. The span-to-height ratio of the shear wall was approximately 0.46 indicating that response is controlled by shearing action. The horizontal load

¹ URGC-Structures, INSA-Lyon, France Email: ile@gcu-beton.insa-lyon.fr

² URGC-Structures, INSA-Lyon, France Email: ile@gcu-beton.insa-lyon.fr

³ ELECTRICITE DE FRANCE - SEPTEN-Villeurbanne Email: Francois.Fleury@edf.fr

⁴ ELECTRICITE DE FRANCE - SEPTEN-Villeurbanne Email: Francois.Fleury@edf.fr

was applied at both sides of the top beam and the bottom beam was fixed to the strong floor. In order to come closer to a pure shear loading condition, a specially designed device was constructed to completely prevent the rotation of the top beam. The differences between each series of tests (T1 to T13) are related to the steel ratio of the reinforcement, the natural frequency of the wall and the vertical loading. The specimen was subjected to excitations in one direction along the axis of the shear wall. A single reference acceleration record was used and each series of tests involved subjecting the test specimen to sequentially increased seismic levels, by varying the intensity of the reference acceleration. The test series No. 5 (T5) was performed with zero vertical loading, the horizontal and vertical steel ratio of the reinforcement being equal to 0.8%. Knowing the design properties of the wall (design stiffness, mass, design shear strength) and making assumption on its damping ratio, the response spectrum method allows to find the seismic level for which the wall could have been designed. Using this procedure, the design acceleration is obtained by multiplying the reference acceleration with a coefficient k :

$$k = \frac{L \cdot e}{M \cdot \Gamma^{dim}(f_0^{dim})} \tau^{dim} \quad (1)$$

where, L is the length of the wall, e is the wall thickness, M is the mass, $\Gamma^{dim}(f)$ is the response spectrum, f_0^{dim} is the design elastic frequency and τ^{dim} is the design shear stress. The design acceleration is then multiplied by an intensity coefficient α . Four increasing acceleration intensity levels were applied for series No. 5 : T5.1 ($\alpha = 1$), T5.2 ($\alpha = 1.3$), T5.3 ($\alpha = 1.5$) et T5.4 ($\alpha = 1.8$).

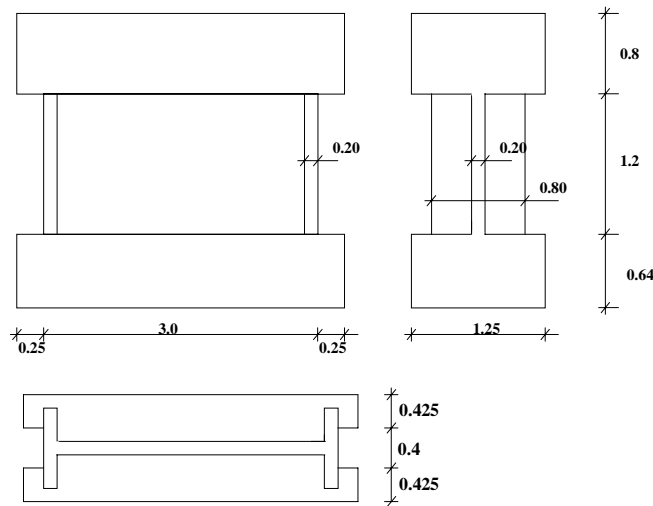


Figure 1: Description of the test specimen (dimensions in m)

MODELLING OF THE TEST SPECIMEN

A two-dimensional (2-D) representation of the specimen was used in this study (Figure 2). The two-dimensional model consists of an equivalent plane mesh representing the different parts of the specimen. As the 2-D representation does not allow for out-of-plane modelling of the flange walls, and thus a single layer of appropriate thickness represented these portions. Four-noded membrane elements were used to model the different parts of the specimen. A discrete modelling is adopted to represent the reinforcement through the use of two-noded truss-bar elements and perfect bond was assumed to exist between concrete and reinforcement. Hence, no explicit bond-slip model was used in the 2-D analysis. A total of 250 membrane elements and 465 truss-bar elements were used, requiring 286 nodes and 572 degrees of freedom. The structure is assumed fully restrained at all nodes along the base of the shear wall, the rotation along the upper edge of the wall being completely blocked. This eliminated the need to model the top and bottom beam and reduced the demands on computation time.

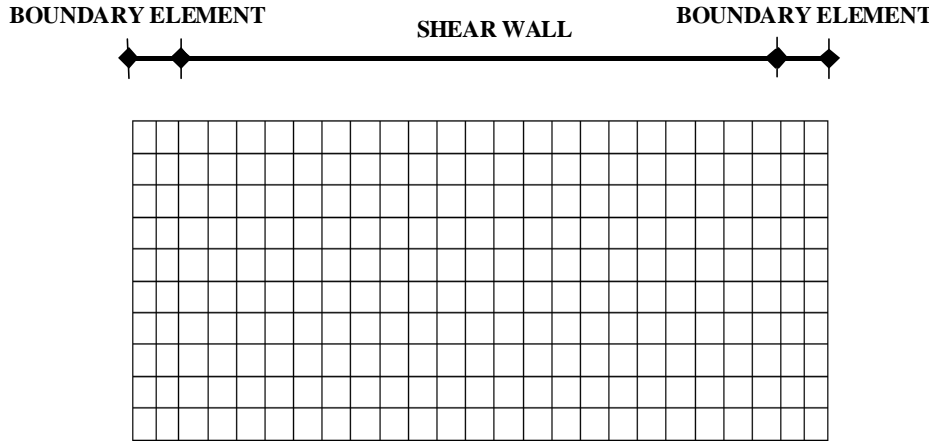


Figure 2 : 2-D Finite element mesh adopted in the analysis

CONCRETE CONSTITUTIVE MODEL

The assumption of a plane state of stress in concrete allows biaxial constitutive models to be used. The INSA's concrete model [Merabet et al., 1995] is based upon the plasticity theory for uncracked concrete with isotropic hardening and associated flow rule. However, only one expression describes the plasticity criterion in tension as well as in compression: this is the Ottosen's criterion. The Ottosen's failure surface (Figure 3) is defined by a unique expression in the space of stresses and has the advantage of being continuous and convex at any point. The normal is therefore always defined and unique, allowing doing away with the choice of the flow direction. Comparison with numerous experimental results shows this criterion to be a good compromise for very different load paths.

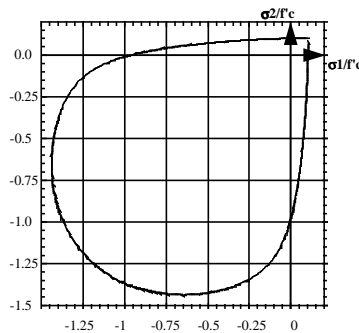


Figure 3: Ottosen's criterion ($f_c/f_t = 0.10$)

For the concrete in tension a smeared fixed crack approach is considered (with a second crack perpendicular to the first one). When the ultimate surface is reached in tension, a crack is created perpendicularly to the principal direction of maximum tension, and its orientation is considered as fixed subsequently. An orthotropic law whose orthotropy directions are normal and parallel to the crack (Figure 4) then models the behaviour. Each direction is then processed independently by a cyclic uniaxial law, and the stress tensor in the local co-ordinate system defined by the direction of the cracks is completed by the shear stress, elastically calculated with a reduced shear modulus (shear retention factor) to account for the effect of interface shear transfer. A constant value of the shear retention factor is adopted up to a value of the crack opening strain equal to $2 \cdot \epsilon_{m}$. For crack opening strain values greater than $2 \cdot \epsilon_{m}$ the shear retention factor is set equal to zero. The uniaxial law implemented in each of the directions allows to account for the main phenomena observed during a loading composed of a small number of cycles. According to the constitutive cyclic law for concrete, as soon as a crack starts to close, the concrete develops some compression, due to the imperfect overlapping of the crack surfaces. Furthermore the model considers damage of the elastic modulus and of the tensile resistance as the inelastic compressive strains increase.

- 1 - Elastic tension
- 2 - Crack opening
- 3, 8 Crack closing
- 4 - Nonlinear compression
- 5, 11 - Damaged unloading, $E_2 \neq E_0$
- 6 - Damaged unloading, Modulus = E_1
- 7 - Reopening of crack
- 9 - Reloading: Linear compression
- 10 - Softening behaviour in compression
- 12 - Elastic tension with resistance $f'_c < f_t$

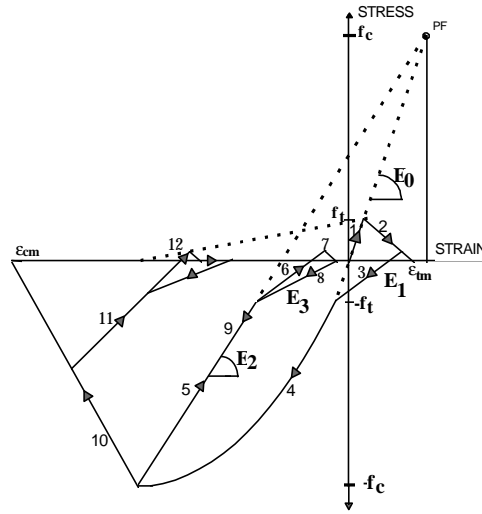


Figure 4: Concrete cyclic law

CRACK MODEL

The relation between stress and crack strain shown on Figure 4 has a linear form and is determined by two parameters, tensile strength f_t and crack opening strain ϵ_{tm} . In unreinforced members, the crack opening strain is determined from fracture mechanics concepts [Bazant and Oh, 1983]:

$$\epsilon_{tm} = \frac{2G_f}{f_t l} \quad (2)$$

where l is the characteristic length of the element in the direction normal to the crack and G_f is the fracture energy for a single crack. The characteristic length l corresponds to a representative dimension of the finite element mesh size and depends on the element type, element size, and element shape and integration scheme. In this study, it is assumed that a good approximation of the characteristic length is obtained if this is related to the area of an element as proposed by Rots [1988]:

$$l = \alpha \sqrt{A_e} \quad (3)$$

in which A_e is the area of the finite element and α is a modification factor that is equal to 1 for quadratic elements and to $\sqrt{2}$ for linear elements. For most practical applications this formulation gives a good approximation, particularly when the finite element mesh is constructed using regular shaped elements. In normally and heavily reinforced members, usually several cracks develop during loading until the cracking process stabilises and stresses are transmitted across cracks through bonded reinforcing. The spacing of cracks at stabilised cracking is determined mainly by the amount of reinforcement. In this study, the concept of released energy and characteristic length is also proposed to model the tension behaviour in diffusely cracked reinforced concrete by introducing the reinforced concrete distributed fracture energy via the formula:

$$G_f^{rc} = G_f + G_f \frac{l}{l_s} \quad (4)$$

where l_s is the average crack spacing at stabilised cracking. The fracture energy of concrete G_f is assumed to be a material parameter according to the [CEB-FIP, 1990] model code. The average crack spacing l_s is a function of the bar diameter, the concrete cover, and the reinforcement ratio and can also be estimated using

recommendations of [CEB-FIP, 1990] model code. The crack opening strain for reinforced concrete members is then given as follows:

$$\varepsilon_{tm} = \frac{2G_f^{rc}}{f_t l} \quad (5) \quad \text{The}$$

procedure outlined above is expected to guarantee the low mesh sensitivity of the response especially for moderately and heavily reinforced elements, as is the case in shear walls with uniform distribution of longitudinal and transverse reinforcing steel.

The material experimental data obtained [Pegon et al., 1998] were used to verify the proposed model. Excepting the value of the initial elastic modulus (which was calibrated in order to obtain the same initial elastic frequency as that obtained at low amplitude vibration tests), all modelling decisions were made before the analysis was executed. The concrete was modelled as having an initial modulus of elasticity of 24 000 MPa and a Poisson ration of 0.20. The concrete compressive strength in the web and boundary element regions was 29.1 MPa and the tensile strength was 1.75 MPa. A shear retention factor of 0.2 was adopted in modelling the shear stiffness of the cracked concrete and the crack opening strain was set equal to 0.001. The descending part of the compressive stress-strain behaviour was approximated by a straight-line function [CEB-FIP, 1990], the corresponding ultimate compressive strain ε_{cm} being equal to 0.006. The steel was assumed as a strain hardening material, with a yield stress of 573 MPa, a tensile strength of 650 Mpa, an elastic modulus of 200×10^3 MPa and an ultimate tensile strain equal to 26.7%.

ANALYSIS RESULTS

The horizontal acceleration signal applied during testing was used as input motion in the analysis. Analysis was undertaken using the program CASTEM 2000, developed at the French Commission for Atomic Energy – CEA [Millard, 1993]. In combination with the ability of this code to save the damage state after each analysis, the four input motions applied during testing (tests T5.1 - $\alpha = 1$, T5.2 - $\alpha = 1.3$, T5.3 - $\alpha = 1.5$ and T5.4 - $\alpha = 1.8$) were considered in chronological order in the analysis. No viscous type of damping was used and all damping was supposed to arise from material hysteretic behaviour. The ability of the orthotropic concrete model to assess the dynamic behaviour of this type of structural element is evaluated by comparison with the available experimental data. The time-history of the calculated horizontal displacements corresponding to tests T5.1 and T5.4 are compared in Figure 5 to 6 with the measured displacements. Similarly Figure 7 to Figure 8 show comparisons of calculated and experimental force-displacement diagrams for the same tests. From Figure 5 it is seen that, for the design input motion (test T5.1), the 2-D representation provides a good agreement with the experimental results, displacement amplitudes and frequencies being correctly predicted. For the highest excitation level (test T5.4) the calculated shape of the displacement curve agrees well with that determined experimentally up to approximately 5.5 sec (Figure 6). After 5.5 sec., as damage increases, the analysis is not able any more to reproduce the experimental results. This seems normal since 3D effects may become very dominant near failure, 2-D models being generally inadequate at this stage. From Figures 7 and 8 it can be seen that, the analysis provides a realistic representation of the stiffness and strength degradation as well as of the pinching behaviour of this type of structure during cyclic loading.

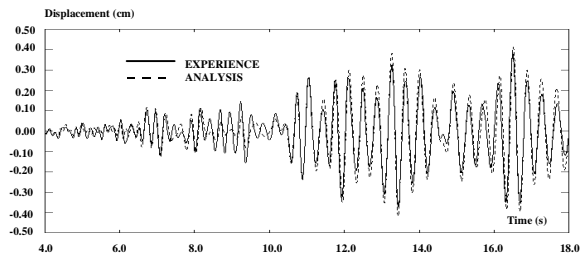


Figure 5: test T5.1 - Top displacement time-history

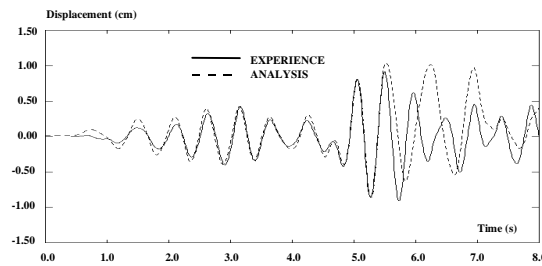


Figure 6: test T5.4 - Top displacement time-history

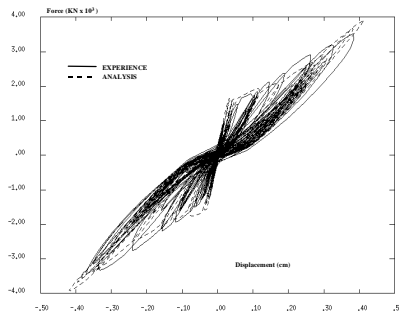


Figure 7: test T5.1 - Force – displacement relationship

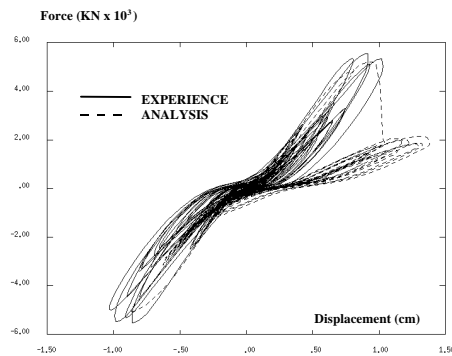


Figure 8: test T5.4 - Force – displacement relationship

For the purpose of assessing the quality of the prediction the calculated maximum values of the top displacement, shear force, frequency drop, dissipated energy and average damping are compared to the experimental response data. The frequency variation during time was calculated using the identification method

proposed at the ELSA Laboratory of ISPRA [Molina and Pegon, 1998]. The maximum frequency drop was then calculated making the difference between the initial (at the beginning of the test) and the final (at the end of the test) natural frequencies. The dissipated energy and the average equivalent damping were evaluated using the area contained in the force displacement hysteretic loops. The following tables summarise the comparison between prediction and experiment.

Table 1 : test T5, Max.values of : displacement, shear force and frequency drop

| TEST T5 | Max. Displacement | | | Max. Shear Force (tons) | | | Max. Frequency drop (Hz) | | |
|-------------|-------------------|----------------|----------------------------------|-------------------------|----------------|----------------------------------|-------------------------------|-----------------------------|--|
| | D ^{exp} | D ^c | D ^c /D ^{exp} | F ^{exp} | F ^c | F ^c /F ^{exp} | Δ _f ^{exp} | Δ _f ^c | Δ _f ^c /Δ _f ^{exp} |
| T5.1 | 0.39 | 0.42 | 1.08 | 352 | 393 | 1.12 | 4.12 | 4.32 | 1.05 |
| T5.2 | 0.65 | 0.56 | 0.86 | 483 | 493 | 1.02 | 0.22 | 0.18 | 0.82 |
| T5.3 | 0.72 | 0.63 | 0.88 | 493 | 408 | 0.83 | 0.13 | 0.08 | 0.61 |
| T5.4 | 0.92 | 1.04 | 1.13 | 554 | 522 | 0.94 | - | - | - |

Table 2 : test T5 – Dissipated energy and average damping

| TEST T5 | Max. Diss. Energy (Jx10 ⁴) | | | Average damping (%) | | |
|-------------|--|----------------|----------------------------------|---------------------|----------------|----------------------------------|
| | E ^{exp} | E ^c | E ^c /E ^{exp} | A ^{exp} | A ^c | A ^c /A ^{exp} |
| T5.1 | 3.46 | 1.99 | 0.58 | 4.79 | 1.77 | 0.37 |
| T5.2 | 7.39 | 3.25 | 0.44 | 4.16 | 1.71 | 0.41 |
| T5.3 | 8.63 | 3.11 | 0.36 | 4.54 | 1.64 | 0.36 |
| T5.4 | 4.77 | 3.33 | 0.70 | 6.61 | 1.25 | 0.19 |

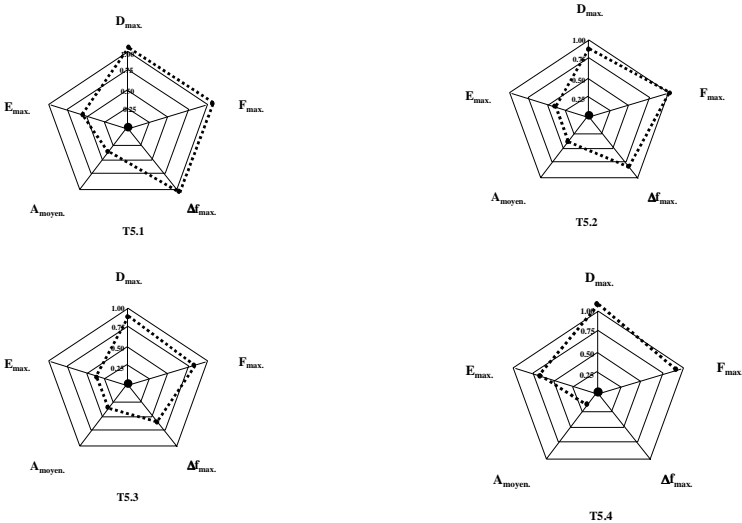


Figure 9 : Radar chart for test T5.1, T5.2, T5.3 and T5.4

These global results are further depicted on the radar charts presented in the Figure 9. These radar charts show that global variables as displacement, force and frequency drop are generally well simulated, but the model is

less successful in predicting the dissipated energy and the average damping. Figure 10 provides the crack pattern predicted at peak displacement during the test T5.4. Compared to the visual observation of cracks the distribution and orientation of cracks in the web portion agrees well with that observed in the test. It is to be noted, however, that vertical cracking in the boundary elements is somewhat overestimated by the 2-D model, due in part to the meshing.

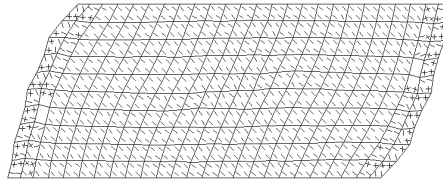


Figure 10: test T5.4: crack pattern at peak displacement

CONCLUSIONS

In this study a constitutive model for predicting the cyclic response of reinforced concrete structures was presented. The model adopts the concept of a smeared crack approach with orthogonal fixed cracks and assumes a plane stress condition. The model is used in the finite element analysis of a shear wall structure that was tested pseudodynamically under a large number of cyclic load reversals due to earthquake loading. The ability of the concrete model to reproduce the most important characteristics of the dynamic behaviour of this type of structural element was evaluated by comparison with available experimental data. The behaviour of the specimens was governed by shear and this type of behaviour represented a severe test of the cyclic constitutive model used in this study. The numerical results showed good correlation between the predicted and the actual response, global response variables as force and displacement being reasonably close to the experimental one, but energy dissipation through repeated cycles was underestimated by the existing model. However, underestimating the energy dissipation leads to conservatism in estimating forces and displacements and hysteretic damage under cyclic loading seems to be less important as far as the force-ductility demand is concerned.

REFERENCES

- Bazant, Z. P., and Oh, B. H., (1983), "Crack band theory for fracture of concrete", *Mat. and Struct.*, Paris, France, **93**(16), pp155-177.
- CEB-FIP, (1990), "Model Code 1990", *Bulletin d'Information*, Lausanne, Switzerland.
- Merabet, O., Djerroud, M., Heinfling, G. and Reynouard, J.M. (1995), "Intégration d'un modèle élastoplastique fissurable pour le béton dans le code Aster", *Contract study EDF/DER, Intermediate Report No. 1/943/001*, National Institute for Applied Sciences, Lyon, France, pp1-49.
- Millard, A. (1993), "CASTEM 2000, Manuel d'utilisation" *Report CEA-LAMS No. 93/007*, Saclay, France.
- Molina, F.J. and Pegon, P., (1998), «Identification of the damping properties of the walls of the SAFE Program», *Technical Note No. I.98.35*, JRC European Commission pp1-16.
- Pegon, P., Magonette, G., Molina, F.J., Verzeletti, G., Dyngeland, T., Negro, P., Tirelli, D., Tognoli, P., (1998), « Safe Programme - Test T5 Report », *Technical Note No. I.98.66*, JRC European Commission pp1-77.
- Rots, J.G. (1988) "Computational modeling of concrete fracture" *PhD thesis*, Delft Univ. of Technol., Delft, The Netherlands, pp1-127.